Ultrafast laser system based on noncollinear optical parametric amplification for laser spectroscopy

Dongjia Han (韩冬佳)[1], Yanyan Li (李妍妍)[1], Juan Du (杜 鹃)[1,*], Kun Wang (王 坤)[2], Yongfang Li (李永舫)[2], Tomohiro Miyatake[3], Hitoshi Tamiaki[4], Takayoshi Kobayashi[5,], and Yuxin Leng (冷雨欣)[1,6,***]**

[1]*State Key Laboratory of High Field Laser Physics, Shanghai Institute of Optics and Fine Mechanics, Chinese Academy of Sciences, Shanghai 201800, China*

[2]*Laboratory of Advanced Optoelectronic Materials, College of Chemistry, Chemical Engineering and Materials Science, Soochow University, Suzhou 215123, China*

[3]*Department of Materials Chemistry, Ryukoku University, Otsu, Shiga 520-2194, Japan*

[4]*Department of Bioscience and Biotechnology, Ritsumeikan University, Kusatsu, Shiga 525-8577, Japan*

[5]*Advanced Ultrafast Laser Research Center, University of Electro-Communications, 1-5-1, Chofugaoka, Chofu, Tokyo 182-8585, Japan*

[6]*FSA Collaborative Innovation Center, Shanghai Jiao Tong University, Shanghai 200240, China*

**Corresponding author: dujuan@mail.siom.ac.cn; **corresponding author: kobayashi@ils.uec.ac.jp; ***corresponding author: lengyuxin@mail.siom.ac.cn*

Received August 25, 2015; accepted October 16, 2015; posted online November 27, 2015

We report the experimental demonstration of transform-limited sub-6 fs pulses at an optimal central wavelength by a tunable noncollinear optical parametric amplification (NOPA) source. Meanwhile, a white light continuum in the near-infrared (NIR) range from 900 to 1100 nm is also successfully generated by focusing the unconverted 800 nm beam during NOPA generation on a sapphire rod. Both visible-pump/visible-probe and visible-pump/NIR-probe experiments are realized using the same laser system. As examples, ultrafast photo-induced exciton dynamics inside two kinds of materials are investigated by the visible-pump/visible-probe and visible-pump/NIR-probe spectroscopy, respectively.

OCIS codes: 140.7090, 320.7150, 320.6629, 300.6530.
doi: 10.3788/COL201513.121401.

Ultrafast optical science is rapidly evolving multidisciplinary fields: it is the ability to excite samples with femtosecond light pulses and probe the subsequent evolution on ultrashort time scales, which completely opens up new fields of research in physics, chemistry, and biology[1–5], particularly for the study of dynamics and reactions in various organic molecules[6–8]. In this kind of research, the dynamics process is required to be from the femtosecond to the picosecond time scale. Therefore, in order to investigate these processes, laser pulses with a shorter duration than the time range of ultrafast dynamics phenomena in the interesting samples are desirable. Most organic materials have absorptions in the visible ranges[9], and sub-15 fs ultrafast visible pulses generated from a tunable noncollinear optical parametric amplification (NOPA) have been widely used to study this kind of real-time spectroscopy for lots of molecules[10–13].

As we know, the available tunability can be used to probe the transient species by photo-inducing optical transitions occurring at various wavelengths[14,15]. The wider the probe spectrum, the more spectral signatures of the transient species involved in the photo process can be monitored simultaneously, which significantly facilitates the assignment of the underlying reaction mechanism. It is of great importance to generate visible-pump/near-infrared (NIR) -probe system for studying the photo-induced dynamics in many photoelectronic materials, because they have strong absorptions in the visible range and the generated electron absorption is in the NIR spectral region[16–18].The alternative approach to cover a much wider range in the NIR is to use a supercontinuum. This well-known phenomenon occurs by focusing an ultrafast laser pulse under the proper conditions into a wide variety of optically transparent nonlinear media, like gases, liquids, photonic crystal fibers, and solids[19]. For example, a femtosecond white-light continuum is available at wavelengths shorter than 1.6 μm, and is generated by a 10 mm cell containing CCl_4 liquids. Meanwhile, a coherent supercontinuum generated from a photonic crystal fiber is applied to an NIR coherent anti-Stokes Raman spectroscopy (NIR-CARS) microscopy, and a clear CARS image of polystyrene microsphere has been obtained using the CH_2-stretching band[20]. Even though white light generation has been used in time-resolved studies, most of the supercontinua obtained from bulk materials are focused on the visible range.

In this Letter, we demonstrate the generation of broad, tunable, sub-6 fs visible pulses by NOPA in a 1 mm-thick type I BBO crystal, and a white-light continuum for the NIR spectral region by a 12 mm-thick sapphire rod is also obtained. These both have very broad and smooth

spectrums, high temporal and spatial coherence, and very high pulse-to-pulse energy stabilities for spectroscopies. Meanwhile, two pump–probe experiments are completed using these two visible-pump/NIR-probe and visible-pump/visible-probe spectroscopies. The results prove that the obtained ultrafast visible pulse and NIR white light continuum are very useful for many kinds of ultrafast time-resolved spectroscopy experiments. They also illustrate that the setup could not only be used to study the visible-pump/NIR-probe spectroscopy, but also visible-pump/visible-probe spectroscopy. Meanwhile, the NIR-probe beam that is generated by the unconverted 800 nm laser pulse of the NOPA system can fully utilize the energy light in the experiment.

A schematic of the experimental pump–probe setup is illustrated in Fig. 1. About 800 μJ after a beam split using a commercial Ti:sapphire regenerative amplifier (0.9 mJ, 50 fs, 5 kHz at 800 nm)[21,22] passes through a 45° fused-silica prism with an incident angle of 49°, a telescope collimates the spectral lateral walk off and images the titled fronts on the focal plane, ensuring the maximum spatial overlap between the pump and the signal fronts. Then, the pulse is frequency doubled in a 200 μm-thick beta barium borate (BBO, type I, $\theta = 29.2°$) crystal. A small fraction of the fundamental energy is converted to generate a continuum of white light seed in a sapphire crystal plate (1 mm thick, used for the visible spectral region). The longer wavelength part in the seed beam is filtered out through a short-pass filter ($T > 90\%$ at 500–750 nm, $R > 99\%$ at 800–850 nm) to prevent any undesired amplification. A pair of chirped mirrors (-25 fs^2/bounce, Layertec) is used to pre-compress and temporally shape the white light, which will have a better overlap with the pump pulse to be amplified in the NOPA. In order to get better beam profiles and higher pulse energies, a two amplification-stage NOPA system (1 mm-thick BBO crystal, type I) is employed with a suitable title angle of 6.4°

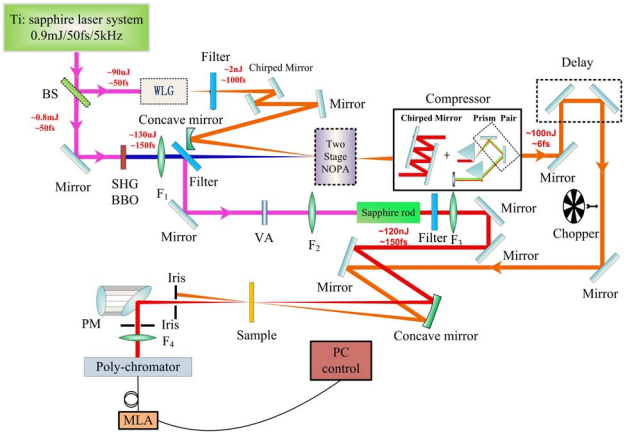

Fig. 1. Schematic of the two-color pump–probe setup. Pulses with 50 fs duration at a 5 kHz repetition rate are used to drive the NOPA and white light generation. BS: beam splitter; SHG: second-harmonic generation; VA: variable attenuator; WLG: white-light generation; MLA: multi-channel lock-in amplifier.

between the seed and the pump. The pulses can be continuously tuned in the spectral region from 510 to 750 nm for the most interesting excitation wavelengths by making a suitable choice for the angle of noncollinearity between the pump and seed, and also by the phase-matching angle of the BBO[23].

The chirped output visible pulses with energies of several microjoules are compressed with a pair of chirped mirrors and Brewster prisms. The easiest way to compress the pulses is by using the fused silica as the prism material, because above 550 nm, the length of the compressor can be substantially shortened with a kind of spectralite flint (SF10) instead of the fused silica prisms. A very helpful feature shown in Fig. 1 is the use of two mirrors acting as a retro reflector inside the prism compressor. This folding allows for a quick and easy adaptation of the length of the compressor to a change of the NOPA center wavelength. In this way, the tunability of the NOPA can really be exploited with a minute change in the alignment of the whole setup. After compression, pulse durations of sub-6 fs can be routinely achieved throughout the visible region. The spectral profile of the output pulse after the prisms at different central wavelengths is shown in Fig. 2(a), and the insert is the compressed pulse duration according to the spectrum represented by the pink line. Meanwhile, the spectral width of the NOPA pulses can be adjusted depending on the specific needs of the spectroscopic experiment. For example, the green line in Fig. 2(a) is the output spectrum which is adjusted according to the absorption spectrum of the zinc chlorin aggregate.

The main mechanism of ultrafast continuum generation is strong self-phase modulation enhanced by the self-steepening of the pulse[24]. In the present study, the Ti:sapphire fundamental is used for the generation of a visible seed continuum by focusing it into a thicker sapphire plate to generate the NOPA beam. We observed that the use of a longer sapphire length ($L = 10$–20 mm) yields a broader continuum, from the visible into the NIR. Therefore, in order to extend the spectra into the NIR to probe the exciton dynamics, we use the white light generated by focusing the unconverted 800 nm beam from the NOPA into a sapphire rod (12 mm thick, used for the infrared spectral region) with a lens F_2 ($f = 500$ mm), as shown in Fig. 1. The unconverted 800 nm beam collected after the second-harmonic generation is used as a pump beam for the visible NOPA in the NIR probe experiment. The specific needs of the spectroscopic experiment should be met by the appropriate choice and alignment of the length of the sapphire rod and filter stage. After the sapphire rod, the white light went through a high-pass filter ($T > 90\%$ above 900 nm, $R > 99\%$ below 900 nm), which can obtain the right spectrum to probe the excited signal and prevent the undesired amplification of the sample. The output spectrum is measured by using lens F_4 ($f = 50$ mm) to image the output surface of the medium onto the entrance slit of the spectrograph. Briefly, the NIR part of the broad and smooth supercontinuum, namely 950–1050 nm, is obtained and shown in Fig. 2(b). To measure

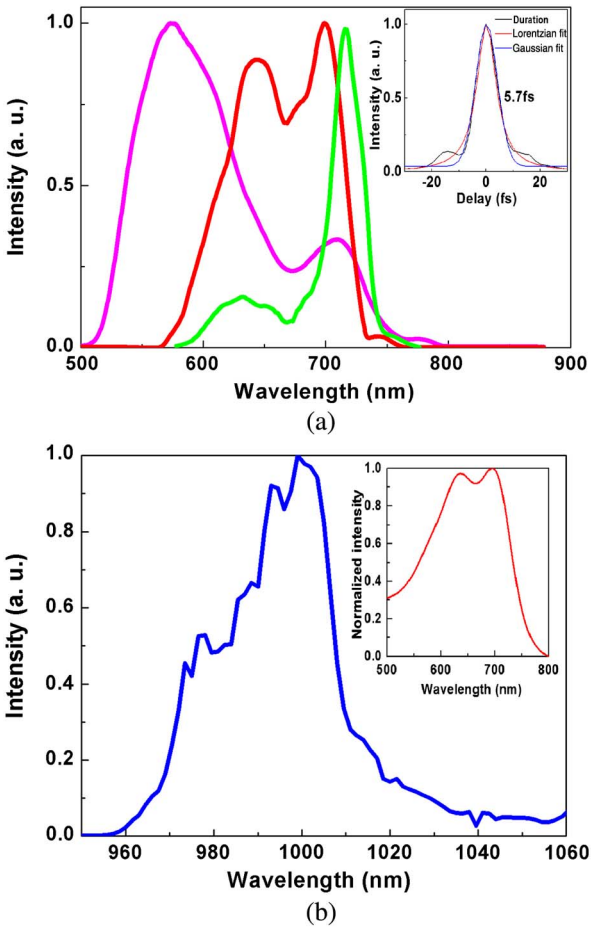

Fig. 2. (a) Spectra of the different visible compressed wavelength pulses. The green line represents the spectra obtained by pumping the zinc chloride aggregate, and the red line represents the spectra for the PTB7-Th polymer in the subsequent experiments. The insert is the shortest compressed pulse duration according to the pink line (the black line is the duration measured, while the red line and blue fit are the Lorentzian fit and Gaussian fit, respectively). (b) Spectra of NIR. Insert is the stationary absorption spectrum of the PTB7-Th polymer (red line).

the pulse at various stages of propagation in the sapphire rod, focusing lens F_2 is moved on a translation stage, such that the desired stage of propagation coincides with the output surface of the medium. Together with the NOPA, the setup allows us to study examples of a typical visible-pump/NIR-probe experiment. Since both the NOPA and NIR beams come from the same laser source, they can synchronize with each other easily. The maximum pulse energy of the NIR-probe beam can be as high as 1 uJ. In this experiment, we do not need the full energy of the NIR beam; we just need to use a 120 nJ energy (150 fs) pulse to probe the sample, since the pump pulse of the visible beam is about 80 nJ at this moment. After passing through the sample at an external angle of ~6° with respect to the pump, the probe is dispersed in a polychromator and guided to a 128-channel lock-in amplifier connected with photodetector[25]. A chopper wheel in the pump beam blocks every second excitation pulse so that changes in the optical density of the sample can be measured.

As an example, the obtained NOPA pulses are divided into two beams and used for a visible-pump and visible-probe experiment. A sample of zinc chloride aggregate[26] is used in this experiment. The pulse energies of the pump and probe are about 30 and 3 nJ, respectively, with spectral range extending from 518 to 786 nm. The time trace of the normalized transmittance changes ($\Delta T/T$) is obtained as a function of the pump–probe time delay from −200 to 2800 fs with every 1 fs step. The experiment is performed at physiologically relevant temperatures (295 ± 1 K). Figure 3(a) shows that the two-dimensional different absorptions ($\Delta A = -\log(1 + \Delta T/T)$) is dependent on the pump–probe time delay in the spectral range between 670 and 780 nm, and the right side shows an example of a ΔA trace. We can observe that the fast relaxation process from the higher multi-exciton state to the one-exciton state is found to take place in 100 ± 5 fs, which shows that only the sub-6 fs ultrafast pulse can

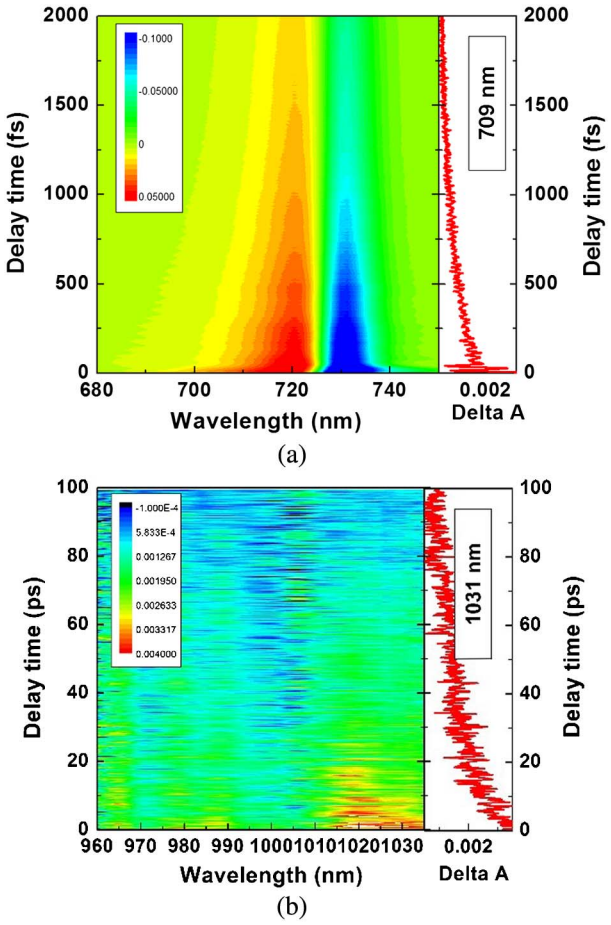

Fig. 3. (a) Two-dimensional pattern of the, different absorbances (ΔA), which are dependent on the time delay from −200 to 2800 fs in the whole probe spectral region (670–760 nm); (right) time trace of different absorbance rates. (b) Two-dimensional pattern of the different absorbances (ΔA) dependent on the time delay from −0.4 to 100 ps in the whole probe spectral region (960–1040 nm); (right) time trace of different absorbances.

accurately detect such a short relaxation time. The detailed analyses have been made in another article[27].

A sample of organic photovoltaic material PTB7-Th polymer[28,29] is used in the visible-pump and NIR-probe experiment. According to the peak absorption of the PTB7-Th polymer, which is shown to be located at around 700 nm in Fig. 2(b), the center wavelength of the pump beam is shifted to be a little longer, as the red line shows in Fig. 2(a), which proves there is a very good overlap between the laser spectrum and the sample absorption spectrum. The pulse energies of the pump and probe beam are 80 and 120 nJ, respectively. The time trace of the normalized transmittance changes ($\Delta T/T$) is obtained as a function of the pump–probe time delay from −0.4 to 100 ps with every 20 fs step. The experiment is performed at physiologically relevant temperatures (295 ± 1 K). Figure 3(b) shows the different absorbance spectra of the exciton dependents the pump–probe time delay in the spectral range between 960 and 1040 nm. On the right is an example of a ΔA trace, and the corresponding decay time of the PTB7-Th polymer is determined to be about 5 ps.

In conclusion, stable sub-6 fs pulses at an optimal central wavelength are obtained using a tunable NOPA source compressed with a pair of chirped mirrors and Brewster prisms. Meanwhile, a white light continuum in the NIR range from 900 to 1100 nm is successfully generated by focusing the unconverted 800 nm beam of the NOPA onto a sapphire rod. The visible-pump/visible-probe and visible-pump/NIR-probe experiments using a zinc chloride aggregate and organic photovoltaic material PTB7-Th polymer as samples are studied with these short pulses, respectively. The results show that the induced absorptions and oscillating features in the time traces of the absorbance change with different periods are clearly observed, which proves that the ultrafast pulses are useful for many kinds of spectroscopy experiments. We believe that the dynamics observed using these kinds of pulses in many materials can potentially be extended to study even more complicated processes, such as energy conversion systems in a natural photosynthesis system, and will provide a good basis to investigate photosynthesis, etc.

This work was partly financially supported by the 100 Talents Program of CAS, the National Basic Research Program of China (Grant No. 2011CB808101), and the National Natural Science Foundation of China (Grant No. 61475169, 61221064).

References

1. G. Cerullo and S. De Silvestri, Rev. Sci. Instrum. **74**, 1 (2003).
2. J. Du, Z. Li, B. Xue, T. Kobayashi, D. Han, Y. Zhao, and Y. Leng, Opt. Express **23**, 17653 (2015).
3. Y. Li, J. Hou, Z. Jiang, and L. Huang, Chin. Opt. Lett. **12**, 031901 (2014).
4. T. Kobayashi, J. Du, W. Feng, and K. Yoshino, Phys. Rev. Lett. **101**, 037402 (2008).
5. Z. Guo, D. Lee, R. D. Schaller, X. Zuo, B. Lee, T. Luo, H. Gao, and L. Huang, J. Am. Chem. Soc. **136**, 10024 (2014).
6. J. Du, Z. Wang, W. Feng, K. Yoshino, and T. Kobayashi, Phys. Rev. B **77**, 195205 (2008).
7. S. M. Falke, C. A. Rozzi, D. Brida, M. Maiuri, M. Amato, E. Sommer, A. De Sio, A. Rubio, G. Cerullo, E. Molinari, and C. Lienau, Science **344**, 1001 (2014).
8. T. Kobayashi, Z. Nie, B. Xue, H. Kataura, Y. Sakakibara, and Y. Miyata, J. Phys. Chem. C **118**, 3285 (2014).
9. J. Liu, Y. Kida, T. Teramoto, and T. Kobayashi, Opt. Express **18**, 4664 (2010).
10. H. Kano, T. Saito, and T. Kobayashi, J. Phys. Chem. B. **105**, 413 (2001).
11. O. A. Sytina, I. H. M. van Stokkum, D. J. Heyes, C. N. Hunter, R. van Grondelle, and M. L. Groot, J. Phys. Chem. B. **114**, 4335 (2010).
12. J. Du, K. Nakata, Y. Jiang, E. Tokunaga, and T. Kobayashi, Opt. Express **19**, 22480 (2011).
13. J. Du, T. Teramoto, K. Nakata, E. Tokunaga, and T. Kobayashi, Biophys. J. **101**, 995 (2011).
14. V. de Waele, M. Beutter, U. Schmidhammer, E. Riedle, and J. Daub, Chem. Phys. Lett. **390**, 328 (2004).
15. U. Megerle, I. Pugliesi, C. Schriever, C. F. Sailer, and E. Riedle, Appl. Phys. B **96**, 215 (2009).
16. U. Schmidhammer, P. Jeunesse, G. Stresing, and M. Mostafavi, Appl. Spectrosc. **68**, 1137 (2014).
17. C. Yi and K. L. Knappenberger, Nanoscale **7**, 5884 (2015).
18. J. Du and T. Kobayashi, Chin. Opt. Lett. **9**, S010601 (2011).
19. R. R. Alfano, *The Supercontinuum Laser Source* (Springer, 2005).
20. V. Nagarajan, E. Johnson, P. Schellenberg, W. Parson, and R. Windeler, Rev. Sci. Instrum. **73**, 4145 (2002).
21. A. Shirakawa, I. Sakane, and T. Kobayashi, Opt. Lett. **23**, 1292 (1998).
22. A. Baltuska, T. Fuji, and T. Kobayashi, Opt. Lett. **27**, 306 (2002).
23. E. Riedle, M. Beutter, S. Lochbrunner, J. Piel, S. Schenkl, S. Spörlein, and W. Zinth, Appl. Phys. B **71**, 457 (2000).
24. G. Yang and Y. R. Shen, Opt. Lett. **9**, 510 (1984).
25. T. Teramoto, J. Du, Z. Wang, J. Liu, E. Tokunaga, and T. Kobayashi, J. Am. Chem. Soc. B **28**, 1043 (2011).
26. T. Miyatake and H. Tamiaki, Coord. Chem. Rev. **254**, 2593 (2010).
27. D. Han, J. Du, T. Kobayashi, T. Miyatake, H. Tamiaki, Y. Li, and Y. Leng, J. Phys. Chem. B. **119**, 12265 (2015).
28. Y. Lin, Z. Zhang, H. Bai, J. Wang, Y. Yao, Y. Li, D. Zhu, and X. Zhan, Energy Environ. Sci. **8**, 1 (2015).
29. P. Cheng, Y. Li, and X. Zhan, Energy Environ. Sci. **7**, 2005 (2014).